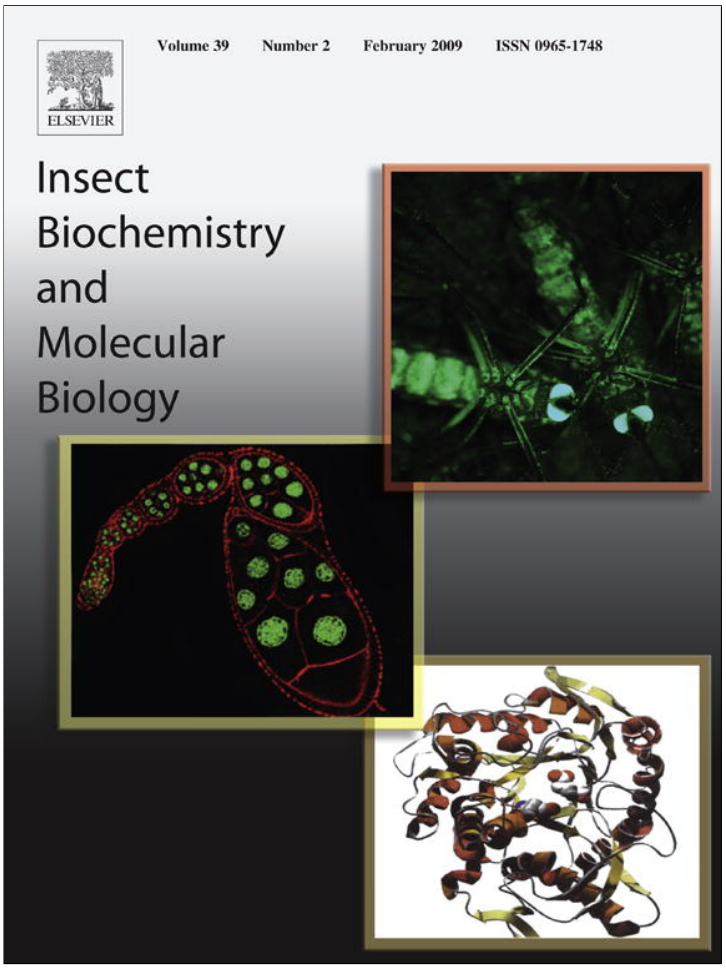

Insect Biochemistry and Molecular Biology 39 (2009) 75–82

Contents lists available at ScienceDirect

Insect Biochemistry and Molecular Biology

journal homepage: www.elsevier.com/locate/ibmb

# Characterization of silk spun by the embiopteran, *Antipaluria urichi*

Matthew A. Collin [a,*], Jessica E. Garb [b], Janice S. Edgerly [c], Cheryl Y. Hayashi [a]

[a] Department of Biology, University of California, Riverside, CA 92521, USA
[b] Arizona Research Laboratories, Division of Neurobiology, University of Arizona, Tucson, AZ 85721, USA
[c] Department of Biology and Environmental Studies Institute, Santa Clara University, Santa Clara, CA 95053, USA

ARTICLE INFO

*Article history:*
Received 9 June 2008
Received in revised form
4 October 2008
Accepted 6 October 2008

*Keywords:*
Biomechanics
cDNA
Fibroin
Silk
Silk glands
Webspinner

ABSTRACT

Silks are renowned for being lightweight materials with impressive mechanical properties. Though moth and spider silks have received the most study, silk production has evolved in many other arthropods. One insect group that has been little investigated is Embioptera (webspinners). Embiopterans produce silk from unique tarsal spinning structures during all life stages. We characterize the molecular and mechanical properties of *Antipaluria urichi* (Embioptera) silk through multiple approaches. First, we quantify the number of silk secretory structures on their forelimbs and the tensile properties of *Antipaluria* silk. Second, we present silk protein (fibroin) transcripts from an embiopteran forelimb protarsomere cDNA library. We describe a fibroin that shares several features with other arthropod silks, including a subrepetitive core region, a non-repetitive carboxyl-terminal sequence, and a composition rich in glycine, alanine, and serine. Despite these shared attributes, embiopteran silk has several different tensile properties compared to previously measured silks. For example, the tensile strength of *Antipaluria* silk is much lower than that of *Bombyx mori* silk. We discuss the observed mechanical properties in relation to the fibroin sequence, spinning system, and embiopteran silk use.



## 1. Introduction

Embioptera, commonly called webspinners or embiids, is an order of insects within Polyneoptera that is most closely related to Phasmatodea, the walking sticks (Terry and Whiting, 2005). There are ~360 named species of embiids (Engel and Grimaldi, 2006) with an estimated diversity of ~2000 species (Ross, 2000). Although webspinners have a worldwide distribution, the majority of species are located within the tropics. Based on the earliest definitive embiopteran fossil, a specimen encased in Burmese amber, the order dates to the mid-Cretaceous. However, because of the derived characters of this fossil, the order is likely to be much older (Engel and Grimaldi, 2006).

Embiopterans are distinctive in their ability to spin silk from unique tarsal organs (Fig. 1A). The forelimb protarsomeres of embiids are greatly enlarged and ultrastructural analysis reveals that these tarsi contain spherical secretory glands. Unlike lepidopterans, which have one pair of silk glands per individual, Ross (2000) estimates that the forelimb tarsi of the webspinner *Oligotoma nigra* have over 300 silk glands (150 per tarsus). The lumen of each embiid silk gland feeds into its own reservoir that has an individual duct leading to a single, hollow, setae-like cuticular process called a silk ejector (Alberti and Storch, 1976; Nagashima et al., 1991). With over 100 silk ejectors per tarsus, embiids can quickly spin extensive networks of silk (Fig. 1B).

Embiopterans use highly choreographed silk spinning behaviors to construct galleries in which they live, forage and reproduce (Edgerly et al., 2002). Galleries consist of dense patches of silken tubes attached to a substrate, such as a tree (Fig. 1) or within leaf litter on the ground. Impressively, galleries that spread over 1 $m^2$ have been documented on trees in the tropics, where embiids graze on lichens and epiphytic algae (Edgerly, 1987a). As fresh food sources are needed, embiids extend the foraging tunnels (Fig. 1C) that radiate outward from a more heavily-silked domicile where embiids typically hide during the day. Investment in silk production by adult females is a significant component of their maternal behavior, a trait that characterizes the order Embioptera. Within a gallery, females lay their eggs and either stitch the eggs into the silk or spin protective silk coverings over the egg clutches (Edgerly, 1987b). Upon emergence, the nymphs can spin silk and continue to do so throughout their lifetime (Ross, 2000).

In this paper, we describe the tensile properties and encoding cDNAs of silk from the embiopteran, *Antipaluria urichi* (Saussure) (Embioptera, Clothodidae) (Fig. 1A). We then compare *Antipaluria* silk to other arthropod silks to identify which features of

* Corresponding author. Fax: +1 951 827 4286.
*E-mail addresses:* matthew.collin@email.ucr.edu, m_collin@earthlink.net (M.A. Collin).

0965-1748/$ – see front matter © 2008 Elsevier Ltd. All rights reserved.
doi:10.1016/j.ibmb.2008.10.004

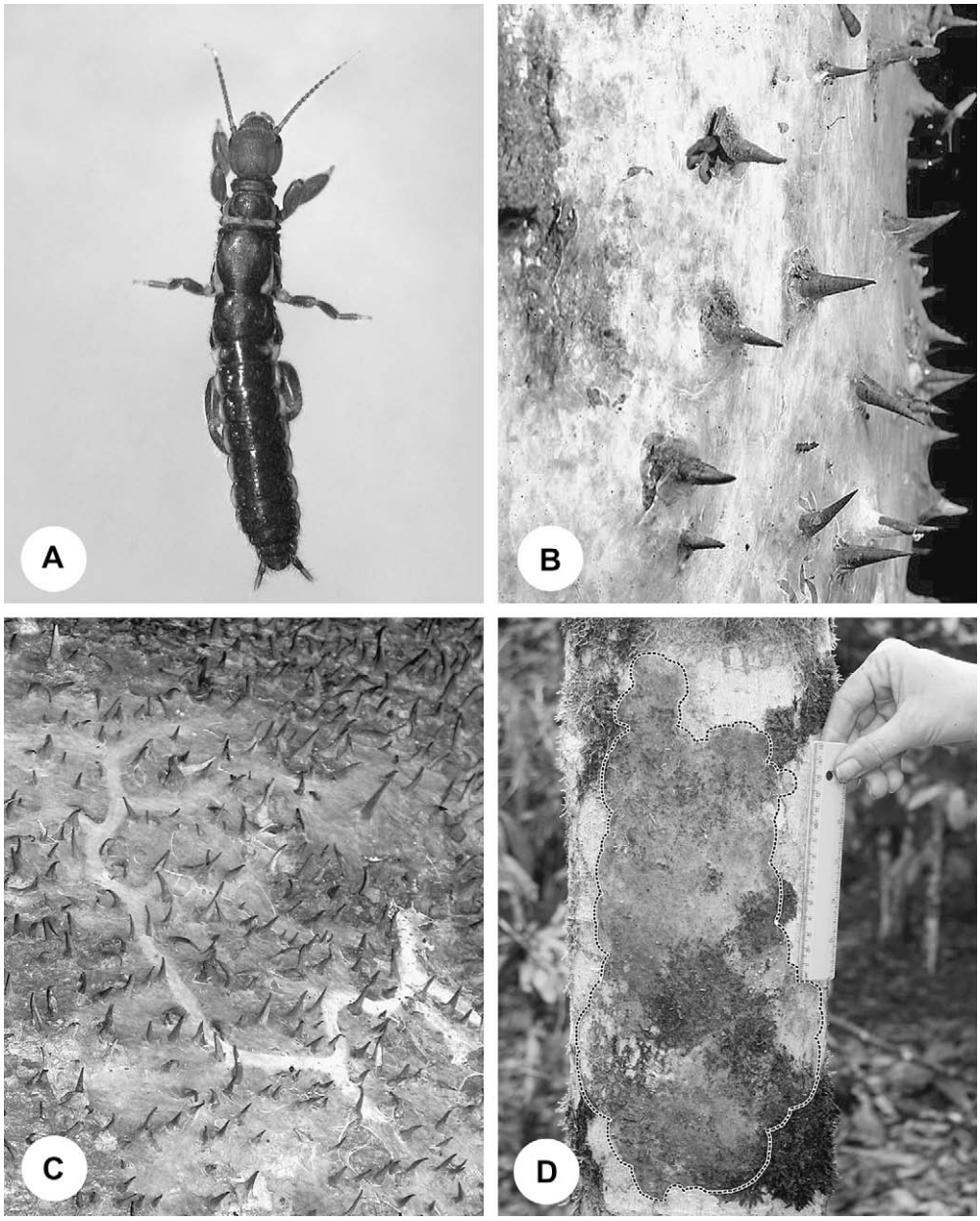


**Fig. 1.** Photographs of *Antipaluria urichi* (Clothodidae) and silk in the field. (A) Adult *Antipaluria* female (body length = 1.5 cm), showing typical embiid traits: elongate, juvenile form and enlarged front tarsi housing silk glands, (B) close-up of a mature colony of *Antipaluria* in Trinidad on thorny bark of *Hura crepitans* (Euphorbiaceae) showing the sheet-like quality of their silk, (C) tube-like galleries spun by *Antipaluria* extending their silk in search of food (epiphytic algae or lichens), and (D) camouflaged sheet-like silk of closely related *Clothoda longicauda* (Clothodidae) of Ecuador (ruler = 15 cm). Silk gallery, circumscribed by the dotted line, is coated with pulverized materials, pieces of moss, and other scraps gathered and incorporated into the silk by the embiids. White patches on the bark are lichens, partially consumed by *Clothoda* (photographs by J.S. Edgerly and E.C. Rooks).

webspinner silk are putatively unique or convergent. For example, some spider and moth silks have sequences that are rich in glycine and alanine (Gatesy et al., 2001). These fibroins can be highly repetitive in amino acid sequence, often being composed of numerous iterations of short subrepeats (Gatesy et al., 2001). Additionally, arthropod fibroins frequently have conserved regions at both the amino- and carboxyl-termini. In spiders, the termini are thought to assist in solubilizing the fibroins within the glandular lumen (Sponner et al., 2005) and in moths, the termini bind other proteins involved in fiber formation (Inoue et al., 2000). Finally, both moth and spider fibers have been shown to be remarkably strong and yet considerably extensible (Gosline et al., 2002). Given the extreme reliance of embiids on their silk, molecular and mechanical characterization of *Antipaluria* silk deepens our understanding of the structure–function relationships of arthropod fibroins.

## 2. Materials and methods

### 2.1. Insect rearing

Embiids were cultured in plastic terrariums containing oak leaves (*Quercus* sp.) and fed romaine or red leaf lettuce. Terrariums were covered with fine mesh nylon (250 μm × 250 μm weave density) to prevent small nymphs from escaping. Cultures were watered two or three times a week with a spray bottle to keep leaf litter moist and maintain humidity.

### 2.2. Ejector number determination

Adult females were anesthetized with $CO_2$ gas and placed in 1.5 mL microfuge tubes filled with 0.15 M sodium chloride, 0.015 M

sodium citrate (SSC) buffer. The tubes were placed in a sonication bath to clean debris from the insects. Specimens were then fixed in 2% gluteraldahyde in SSC buffer for 2 h, followed by five washes in fresh SCC buffer. The insects were then placed in 1% osmium tetroxide in SSC for 2 h. After rinsing with fresh SSC buffer, the specimens were dehydrated in increasing concentrations (30–100%) of ethanol and stored in 100% ethanol.

Fixed specimens were critical point dried in a Balzers CPD0202 (BAL-TEC AG, Liechtenstein) and then coated with gold palladium in a Cressington 108 AUTO (Cressington Scientific Instruments Ltd, Watford, UK) sputter coater. A Phillips XL30 FEG (FEI Co., Hillsboro, OR, USA) scanning electron microscope was used to image tarsi. Pictures were taken of the whole plantar tarsal surface (57×, Fig. 2A) and at increased magnification (449×, Fig. 2B).

The number of ejectors was estimated from the SEM images using ImageJ software (Abramoff et al., 2004). Starting with a single, high quality 449× image (Fig. 2B), the number of individual ejectors was counted. The area of the 449× image was then computed by multiplying the scaled length and width of the photo. The total tarsal surface area was determined from the whole tarsus image (57×) by using the ImageJ polygon area tool to trace around the edges of the tarsus. By dividing the total tarsal surface area by the 449× image area, the number of 449× images that would fit within the total tarsal area was calculated. This number was multiplied by the ejector count from the 449× image to estimate the total number of ejectors per tarsus.

### 2.3. Silk collection

Individual embiids (adults) were anesthetized using $CO_2$ gas and placed on their dorsal side atop a dissection microscope stage. C-shaped cards with 0.5 cm gaps (distance between the two arms) were dragged across a webspinner's tarsus to obtain silk fibers. Small drops of cyanoacrylate were dabbed on each arm of the C-shaped card to affix the silk sample. Each sample card was inspected with a compound light microscope at 100× and 1000× magnification, to determine the number of fibers spanning the gap. Cards with more than four fibers were discarded because of the intractability of distinguishing individual fibers for diameter measurements.

### 2.4. Tensile testing

Silk sample diameters were measured using polarized light microscopy (Blackledge et al., 2005). Accuracy of the polarized light microscope measurements was confirmed using scanning electron microscopy on exemplar fibers (data not shown). Tensile tests were performed on a Nano Bionix® tensile tester (MTS Oakridge, TN, USA). Silk sample cards were mounted to the clamps of the tensile tester and connecting card material was removed such that only silk spanned the gap between the clamps. Fibers were axially stretched at a strain rate of 1% per second until failure. Tests were conducted at room temperature, which ranged from 23 to 26 °C, and relative humidity of 26 to 32%. Measurements collected included: tensile strength (true stress), the force needed to stretch a fiber to breaking; extensibility (true strain), the maximum elongation at breaking; stiffness, the material's resistance to stretching; and toughness, the amount of energy a given volume of material can absorb before breaking.

### 2.5. Silk cDNA characterization

Twenty adult female embiids were used for tissue collection. Live insects were anesthetized with $CO_2$ gas prior to removal of whole forelimb tarsi. The tarsi were excised at the joint between the first and second segments such that only the silk producing part of the forelimb was removed. The tarsi were immediately flash frozen in liquid $N_2$ and stored at −80 °C.

Frozen tarsi were homogenized in TRIzol reagent (Invitrogen, Carlsbad, CA, USA) for RNA extraction. Total RNA was purified using the RNeasy mini kit (Qiagen, Valencia, CA, USA) and mRNA was pooled from total RNA using oligo $(dT)_{25}$ magnetic beads (Invitrogen, Carlsbad, CA, USA). cDNA synthesis followed the Superscript II protocol (Invitrogen, Carlsbad, CA, USA) using an anchored oligo $(dT)_{18}V$ primer. The resulting cDNA were then size-selected with a ChromaSpin 1000 (Clontech, Mountain View, CA, USA) column and ligated into pZErO-2 plasmid (Invitrogen, Carlsbad, CA, USA) at the EcoRV site. The plasmids were electroporated into TOP10 *Escherichia coli* cells (Invitrogen, Carlsbad, CA, USA). Approximately 1800 recombinant colonies were arrayed into a cDNA library. The library was replicated onto nylon membranes. One third of the library was assayed to determine insert size (Beuken et al., 1998). Clones with inserts greater than ~600 bp were chosen for sequencing. The entire library was screened with a $\gamma$-$^{32}$P radiolabeled probe (5′-CCA GAK CCT GAK CCT GCA CC-3′) designed from a putative fibroin cDNA discovered amongst the size-selected clone sequences.

Size-selected and probe positive clones were sequenced with the universal primers, T7 and Sp6, at the Core Instrumentation Facility at the University of California, Riverside. DNA sequences were translated using Sequencher 4.2 (Gene Codes, Ann Arbor, MI, USA) and submitted for BLASTX searches against the nr database (http://www.ncbi.nlm.nih.gov/BLAST). Predicted translations and codon usage analyses were performed in MacVector 7.0 (Oxford Molecular Group, Oxford, UK).

### 2.6. Amino acid analysis

Embiids were placed in petri dishes and allowed to spin silk. Silk samples were collected and sent to the Molecular Structure Facility

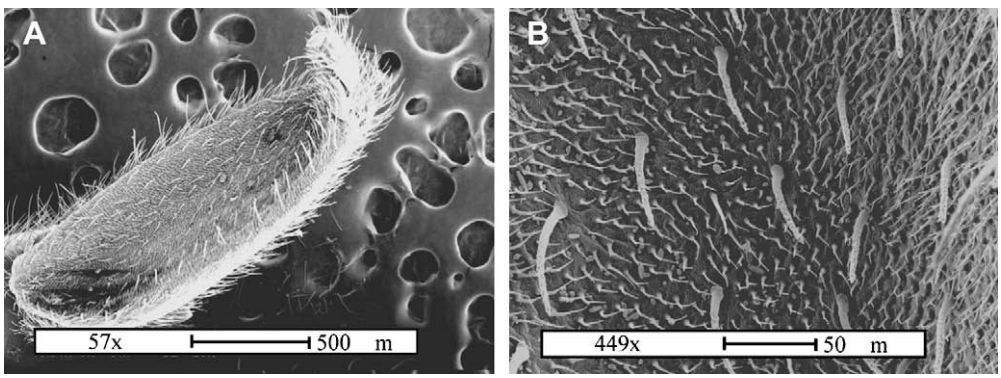


**Fig. 2.** SEM images of *Antipaluria* tarsus. (A) Whole *Antipaluria* tarsus and (B) higher magnification image of tarsal ventral surface showing prominent silk ejectors.

at the University of California, Davis. The samples were hydrolyzed in 6 N HCl, 0.1% phenol at 110 °C for 24 h. Molar fractions were determined on a Hitachi L-8800 (Hitachi Ltd., Tokyo, Japan) amino acid analyzer using ion exchange chromatography followed by ninhydrin reaction detection.

### 2.7. Northern blot hybridization

Total RNA was extracted using the methods described in Section 2.5, from the forelimb tarsi of six *Antipaluria* females. Total RNA was also extracted from a female that was intact except that her forelimb tarsi had been removed. Ten microliters of total RNA was loaded into a 1.2% agrose gel with 3% formaldehyde. Equal loading of RNA samples and Ambion RNA Millennium markers (Ambion, Austin, TX, USA) were visualized using methylene blue staining. Northern blot procedure followed Ding et al. (1995) and the membrane was probed with the same oligonucleotide as the cDNA library (see Section 2.5). The membrane was exposed to a phosphor screen overnight and imaged on an Amersham Typhoon 9410 scanner (Amersham Biosciences, Piscataway, NJ, USA).

## 3. Results and discussion

### 3.1. Ejector number determination

Silk producing organs vary widely across arthropod lineages. For example, spiders spin silk from abdominal glands, moths produce silk from modified salivary glands, and beetle larvae secrete silk from malpighian tubules (Craig, 1997). To visualize the details of the embiopteran silk production apparatus, we examined the *Antipaluria* silk spinning organ with SEM. Numerous silk ejectors were observed in the SEM image of the ventral tarsal surface (Fig. 2A). The total tarsal surface area determined from Fig. 2A was 0.775 $mm^2$. From Fig. 2B, the number of ejectors was estimated by counting the longer, setae-like projections on the tarsal surface. Given the total area of Fig. 2B (50,647.8 $\mu m^2$) and the number of ejectors in that area (15), there are approximately 230 ejectors per tarsus. This results in an ejector density for the ventral tarsal surface of roughly one ejector per 2900 $\mu m^2$. Assuming that each ejector is fed by its own silk gland, then *Antipaluria* has ~230 silk glands per tarsus. In comparison to the ~150 silk glands per *Oligotoma nigra* tarsus (Ross, 2000), *Antipaluria* has 1.5× more glands. This suggests that the number of silk glands in embiids may roughly scale with body length because *Antipaluria* is 1.6× longer than *Oligotoma* (Ross, 1957; Edgerly, 2002). Other factors that may contribute to the difference in ejector number could be the relationship of tarsal dimension to body size and variation in ejector density among species.

We determined that the mean diameter of an *Antipaluria* silk fiber is 0.805 ± 0.324 μm (SD), which is towards the lower end of the reported 0.1–11.5 μm range of arthropod silk diameters (Pérez-Rigueiro et al., 1998; Young and Merritt, 2003; Blackledge and Hayashi, 2006b). Despite the minute size of its fibers, *Antipaluria* can readily spin large quantities of silk due to the impressive number of ejectors on their tarsi (~460 total per individual).

Tarsal silk production has independently evolved in tarantulas (Gorb et al., 2006) and dance flies (Young and Merritt, 2003). In addition to their abdominally produced silks, the Costa Rican zebra tarantula (*Aphonopelma seemanni*) secretes silk through tarsal ejectors that assist these spiders during locomotion (Gorb et al., 2006). Tarantula tarsal silk is secreted as a liquid and then solidifies quickly to prevent the animal from falling while climbing a vertical surface (Gorb et al., 2006). In contrast, embiid silk appears to be secreted as a dry fiber and is not used in an adhesive fashion (Beutel and Gorb, 2001).

Silk production is sexually dimorphic in dance flies (Empidinae). Adult males use tarsal silk to ball algae and prey insects into packages, and then present these bundles to females as a prelude to mating (Young and Merritt, 2003). The male's enlarged basitarsus has 12 pairs of glands with each ejector producing silk fibers up to 3 μm in diameter (Young and Merritt, 2003). The spinning apparatuses of dance flies and embiids may be of similar developmental origin. For example, Sutherland et al. (2007) note that both embiopterans and dance flies produce silk through class III dermal glands. Additionally, in both taxa, tarsal silk glands have been hypothesized to be evolutionarily derived from modified sensory organs (Merritt, 2007). However, the enlarged tarsi of a dance fly contain few silk glands surrounded by large volumes of hemolymph (Young and Merritt, 2003), while webspinner forelimb tarsi are entirely filled with over a hundred silk producing glands (Nagashima et al., 1991).

### 3.2. Tensile properties

The impressive and diverse mechanical properties of arthropod silks have generated great interest in exploring their potential to inspire new types of high-performance biomimetic materials (Fedič et al., 2003; Chang et al., 2005; Blackledge and Hayashi, 2006b; Swanson et al., 2006; Sutherland et al., 2007). For example, some spider silks are tougher than steel or Kevlar, while others can extend over 200% (Gosline et al., 2002). Independently evolved arthropod silks are likely to have different mechanical properties because of lineage-specific secretory mechanisms, molecular compositions, spinning behaviors, and ecological functions (e.g., pupation, dispersal, prey capture, predator avoidance, reproduction). Given the importance of silk to organismal fitness, it is expected that silk performance has been optimized through natural selection.

We tensile tested 12 *Antipaluria urichi* silk samples. The resulting stress–strain curves are characteristic of viscoelastic materials, such as linear polymers and tendons, that at first resist applied forces like a solid (initial slope of the stress–strain curve) and then reach a yield point exhibited by a change in slope (Fig. 3). After the yield point, the silk fiber behaves more like a viscous material and stretches until breaking.

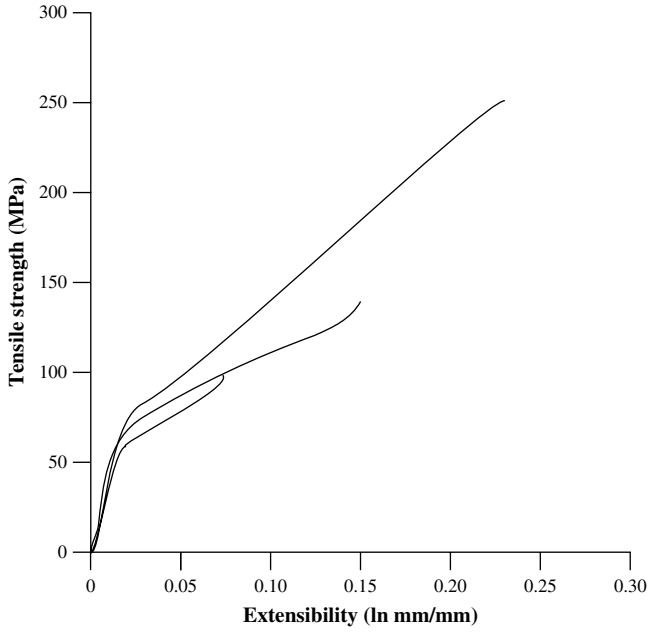


**Fig. 3.** Three representative stress–strain curves of *Antipaluria* silk tensile tests that depict the maximum, median, and minimum true stress values.

The extensibility of webspinner silk is comparable to that of *Bombyx* (silkworm) and *Kahaono* (leafhopper) silks (Table 1). These distantly related insects all employ their silks to build protective structures. Besides extensibility, silk stiffness may serve an important role in webspinner defense. Breaching a woven silk sheet by puncturing or pulling is dependent on the stiffness of the material (Termonia, 2006). Since many organisms that feed upon webspinners tear the silk sheets to obtain their prey, silk stiffness may be critical to impede predators and provide time for the embiids to flee. Leafhoppers and silkworms also use their silk to create protective structures, hence we hypothesize that similarity of function has led to roughly equivalent stiffness values (Table 1).

While the extensibility and stiffness of *Antipaluria* silk is comparable to other arthropod silks, the tensile strength of webspinner silk is markedly lower (Table 1). Because toughness is a characteristic dependent on extensibility, stiffness, and strength (quantified by the area under the stress–strain curve, Fig. 3), the weak strength of embiid silk results in modest toughness. Embiids simultaneously spin hundreds of fibers to construct their galleries and, to our knowledge, never suspend themselves with silk. Spiders and moths however, use paired filaments for high tensile, energy absorbing applications such as orb-weaving spiders capturing flying insects with aerial webs (Blackledge and Hayashi, 2006a) or caterpillars releasing an escape line to drop quickly from predators (Sugiura and Yamazaki, 2006). Thus, in contrast to these arthropod silks, it is likely that embiid silk is not under selection for high tensile strength or toughness.

### 3.3. Amino acid sequence

We found six clones in our cDNA library that encode the same putative silk protein. The longest clone had 753 nucleotides of coding sequence and included the stop codon. These clones were identified based on sequence similarity to other arthropod silks. Specifically, as with a number of known silks, the predicted translation of the *Antipaluria* fibroin cDNA was primarily composed of glycine, serine and alanine (Fig. 4A; accession no. FJ361212). The predicted amino acid composition of the putative fibroin closely matched the empirically determined amino acid composition of spun silk (Fig. 5). The slight discrepancy between the molar percentages of spun silk and the fibroin cDNA translation is possibly due to the cDNA being partial length and lacking amino-terminal coding sequence. Additionally, the presence of other proteins in spun silk may partially explain the difference. Moth silks, for example, are known to be composed of accessory proteins as well as fibroins (Žurovec et al., 1998; Nirmala et al., 2001).

Examining the *Antipaluria* fibroin cDNA in more detail, it is evident that strings of codons appear in highly repetitive groupings (Fig. 4A). A particular group of codons (GGT GCA GGA TCA GGC TCT) appears six times within the sequence. Dominating the fibroin sequence are 21 variants of this codon motif, 17 of which differ by two nucleotides or less. This codon motif encodes Gly-Ala-Gly-Ser-Gly-Ser, the most prevalent peptide motif in the fibroin.

Codon usage within the fibroin cDNA is highly skewed (Table 2). There is a strong preference for glycine, alanine, and serine codons to have thymine (T) and adenosine (A) located in the third nucleotide position. This same pattern has been observed in convergently evolved silks (Ayoub et al., 2007; Sutherland et al., 2007). Some causes suggested for codon usage bias include adaptation to tRNA frequencies within the cytoplasm (Rocha, 2004) and mutational bias of the organism towards particular transitions and transversions (Murray et al., 1989). Another reason would be to reduce frame shift mutations. Given the repeated codon motifs in the *Antipaluria* fibroin cDNA described above, the embiid silk gene has attributes similar to microsatellites. Changes in microsatellite repeat number often occur because of mutational events, such as slip-strand mispairing (Taylor and Breden, 2000). In coding sequence, slip-strand mispairing could result in a deleterious frameshift. Given the importance of silk to embiid fitness, mechanisms that reduce frameshift mutations within the sequence would be beneficial. The observed codon usage bias (Table 2) might act as a mechanism to reduce frameshifts in repetitive fibroin genes. Without the interspersed Ts and As in the glycine, alanine, and serine codons, the gene sequence would be dominated by cytosine (C) and guanine (G) bases. A G/C rich sequence is expected to experience frequent frameshifts because Gs and Cs can partner anywhere along the length of the sequence. Because of codon usage bias, the *Antipaluria* fibroin transcript is not G/C rich and the distribution of Ts and As may help the sequence remain in frame after slip-strand mispairing or unequal crossover events. If such mutations occurred within a silk sequence, then variation in the length of silk genes would be observed among individuals. In fact, allelic variants of spider and silkworm fibroin genes have been observed that are akin to the length variations seen in microsatellite loci (Ueda et al., 1985; Higgins et al., 2007). Similar allelic variation is expected in the webspinner silk gene.

We observed similarities between the repetitive regions of the webspinner fibroin and the *Bombyx mori* heavy chain (HC) fibroin repetitive region (accession no. NM_001113262). Both silks are composed of short repeats of glycine, serine, and alanine (Fig. 4B). Iterations of glycine–alanine couplets and poly-alanine repeats are thought to form β-crystalline structures, which contribute to tensile strength (Warwicker, 1960; Hayashi et al., 1999; Fedič et al., 2003; Lawrence et al., 2004; Trancik et al., 2006). Craig (1997) hypothesized that webspinner silk contains crystallites based on sheering forces that occur during spinning. Our sequence results are consistent with this hypothesis. Despite the similarity in their protein sequences, *Antipaluria* silk is weaker than *Bombyx* silk. This performance difference may result from disparities in the percentage of β-sheet secondary structure, crystallite size (Termonia, 1994), or molecular weight (Termonia et al., 1985; see below).

The carboxyl-terminal region of the embiid fibroin has features observed in many other silks (Fig. 4C; Sehnal and Žurovec, 2004;

**Table 1**
Tensile properties of *Antipaluria* silk and other arthropod silks.

| | Tensile strength (MPa) | Extensibility (ln mm/mm) | Stiffness (GPa) | Toughness (MJ/m$^3$) |
|---|---|---|---|---|
| *Antipaluria* ($N = 6$, $n = 12$) | $158.4 \pm 43.3$[a] | $0.134 \pm 0.08$[a] | $5.9 \pm 2.4$[a] | $13.9 \pm 8.5$[a] |
| *Hydropsyche* (caddisfly) | $221 \pm 22$[a] | $1.16 \pm 0.10$[a] | – | – |
| *Kahaono* (leafhopper) | $280 \pm 72$ | $0.069 \pm 0.01$ | $4.4 \pm 1.6$ | – |
| *Bombyx* (silkworm) | 600 | 0.18 | 7 | 70 |
| *Kukulcania* (house spider) | $830 \pm 6$[b] | $0.26 \pm 0.014$[b] | $22.2 \pm 1.52$[b] | $132.2 \pm 7.53$[b] |
| *Araneus* (orb-weaving spider) | $1050 \pm 5$[b] | $0.29 \pm 0.014$[b] | $8.3 \pm 0.54$[b] | $141.2 \pm 0.77$[b] |

*Hydropsyche*, Brown and Ruxton, 2004; *Kahaono*, Chang et al., 2005. *Bombyx*, Gosline et al., 1999; *Kukulcania* and *Araneus* draglines, Swanson et al., 2006. For *Antipaluria*, $N$ = number of individuals from which silks were tested and $n$ = number of tests.

[a] Standard deviation.

[b] Standard error of mean.

**A** *Antipaluria* fibroin repetitive region

```
TCA GGA TCT GGC TCT GGT GCA GGA TCA GGC TCT GGT GCA GGA TCA GGC TCT GGT GCA GGA TCA GGC
Ser Gly Ser Gly Ser Gly Ala Gly Ser Gly Ser Gly Ala Gly Ser Gly Ser Gly Ala Gly Ser Gly

TCT GGT GCA GGA TCA GGC TCT GGT GCA GGA TCA GGC TCT GGT GCA GGA TCA GGT GCA GGG TCA GGA
Ser Gly Ala Gly Ser Gly Ser Gly Ala Gly Ser Gly Ser Gly Ala Gly Ser Gly Ala Gly Ser Gly

TCT GGT GCA GGC TCA GGA TCT GGT GCA GGG TCA GGA TCT GGT GCA GGC TCA GGA TCT GGT GCA GGC
Ser Gly Ala Gly Ser Gly Ser Gly Ala Gly Ser Gly Ser Gly Ala Gly Ser Gly Ser Gly Ala Gly

TCA GGA TCT GGT TCA GGT AGT GGA TCA GGA TCC GGC TCT GGT GCA GGA TCA GGC TCA GGA TCT GGT
Ser Gly Ser Gly Ser Gly Ser Gly Ser Gly Ser Gly Ser Gly Ala Gly Ser Gly Ser Gly Ser Gly

GCT GGC TCA GGT GCA GGA TCA GGC TCT GGT GCA GGC TCA GGA TCA GGT TCA GGC TCA GGA TCT GGT
Ala Gly Ser Gly Ala Gly Ser Gly Ser Gly Ala Gly Ser Gly Ser Gly Ser Gly Ser Gly Ser Gly

GCA GGC TCA GGT TCT GGA TCA GGT GCA GGC TCA GGA TCT GGT GCA GGT TCA GGC TCA GGA TCT GGT
Ala Gly Ser Gly Ser Gly Ser Gly Ala Gly Ser Gly Ser Gly Ala Gly Ser Gly Ser Gly Ser Gly

GCA GGC TCA GGT TCT GGA TCA GGT TCT GGT AGT GGA TCA GGA TCT GGT TCA GGT GCA GGT
Ala Gly Ser Gly Ser Gly Ser Gly Ser Gly Ser Gly Ser Gly Ser Gly Ser Gly Ser Gly Ala Gly

TCT GGT GCA GGA TCA GGT GCA GGC TCT GGA TCA GGC GCA GGC TCA GGT TCT GGA TCA GGA TCT GGT
Ser Gly Ala Gly Ser Gly Ala Gly Ser Gly Ser Gly Ala Gly Ser Gly Ser Gly Ser Gly Ser Gly

GCA GGT TCA GGA TCA GGA TCT GGT TCA GGT AGT GGA TCA GGA TCT GGT GTA GGC TCA GGT GCT GGA
Ser Gly Ser Gly Ser Gly Ser Gly Ser Gly Ser Gly Ser Gly Ser Gly Ser Gly Val Gly Ser Gly Ala Gly

TCA GGT TCA GGA TCA GGC TCA GGT TCA GGC TCA GGA TCA GGT TCA GGA TCT GGA GGT
Ser Gly Ser Gly Ser Gly Ser Gly Ser Gly Ser Gly Ser Gly Ser Gly Ser Gly Ser Gly Gly
```

**B** Representative fibroin repetitive regions

```
Antipaluria GAGSGSGAGSGSGAGSGAGSGSGAGSGSGA
Bombyx      GAGSGAASGAGSGAGAGSGAGAGSGAGAGS
```

**C** Fibroin carboxyl-terminal regions

```
Antipaluria DSGEIDCPVPADLYDSNDWDAIDAYVERYC
Bombyx      DYSRRNVRKNCGIPRRQLVVKFRALPCVNC
```

**Fig. 4.** *Antipaluria* fibroin partial-length cDNA sequence and translation (accession no. FJ361212). (A) Nucleotides (one-letter abbreviations) grouped into codons with amino acid (aa) translation (three-letter abbreviations) beneath. (B) Exemplar repetitive regions of *Antipaluria* fibroin and *Bombyx mori* heavy-chain fibroin (accession no. NM_001113262) shown by one-letter aa abbreviations. (C) Fibroin carboxyl-terminal regions shown by one-letter aa abbreviations. Glycine, serine, and alanine are shown in green, blue, and red, respectively. Cysteine is purple and boxed.

Garb et al., 2006; Ittah et al., 2006; Ayoub et al., 2007). One such feature is the non-repetitive and hydrophilic nature of the carboxyl-terminal region (Fig. 4C). It has been hypothesized that the hydrophilic amino acids in this region aid in the solubility of silk proteins in the glandular lumen (Sponner et al., 2005). Another possibly convergent feature of the webspinner fibroin carboxyl-terminal region is the presence of cysteine residues (purple and boxed in Fig. 4C). In *Bombyx* and other lepidopteran HC fibroins, similarly positioned cysteine residues form disulfide bonds that join silk monomers (Inoue et al., 2000; Yonemura and Sehnal, 2006). Additionally, spider major ampullate silk has a conserved carboxyl-terminal cysteine that has been demonstrated to be important in protein–protein interactions leading to fiber formation (Ittah et al., 2006). Given the importance of the carboxyl-terminal region in silk fiber formation and the observed similarities across divergent taxa, we hypothesize that these features can be explained by convergence. We suggest that due to the analogous placement of cysteines in the *Antipaluria* fibroin, these residues may play a key role in fiber formation. As more webspinner fibroins are characterized, it is expected that their carboxyl-terminal regions will contain the highly conserved cysteine residues.

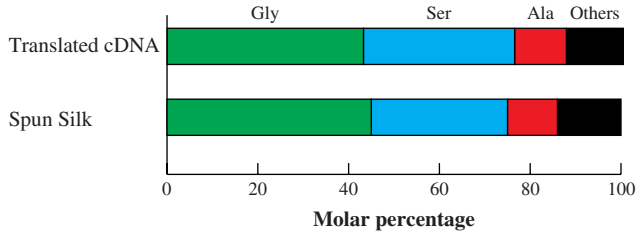


**Fig. 5.** Predicted amino acid composition of the translated *Antipaluria* fibroin cDNA in comparison to the empirically determined composition of *Antipaluria* spun silk. Molar percentages of glycine, serine, alanine, and all other amino acids are shown in green, blue, red, and black, respectively.

### 3.4. Northern blot

The transcript size of the *Antipaluria* silk fibroin is in the range of 1.5 to 2.5 kb (Fig. 6). The lack of a narrow, sharp band may be due to overexposure because the probe, which was specific to the repetitive coding region, hybridizes numerous times within each fibroin transcript. Alternatively, the indistinct band on the blot image may result from the necessity to use multiple individuals to acquire enough total RNA. Individuals may vary in transcript length, as would be consistent with the hypothesis that fibroin genes can readily change length because of their microsatellite-like sequence characteristics (Garb and Hayashi, 2005; Ayoub et al., 2007).

The determination of the *Antipaluria* fibroin transcript size provides insight regarding the observed tensile strength. Theoretical and empirical studies of synthetic polymers have shown that strength is greatly affected by the molecular weight of the

**Table 2**
Molar percentage and codon usage for the most common amino acids (aa) in the predicted translation of the *Antipaluria* fibroin cDNA.

| aa | % aa | Codon | % Codon |
|---|---|---|---|
| Gly | 44 | GGA | 36 |
| | | GGC | 23 |
| | | GGG | 2 |
| | | GGT | 39 |
| Ser | 34 | AGC | 1 |
| | | AGT | 5 |
| | | TCA | 58 |
| | | TCC | 1 |
| | | TCG | 0 |
| | | TCT | 35 |
| Ala | 12 | GCA | 86 |
| | | GCC | 0 |
| | | GCG | 0 |
| | | GCT | 14 |

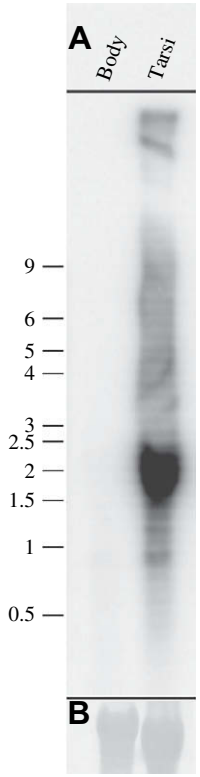


**Fig. 6.** Northern blot analysis of the *Antipaluria* fibroin transcript. (A) Tarsal-specific expression of transcript with sizes (in kb) indicated on the left. (B) Verification of equal loading of RNA in each lane using ribosomal bands visualized with methylene blue stain, scanned in black and white.

monomers (Termonia et al., 1985; Hallam et al., 1986). Larger monomeric subunits increase tensile strength through greater molecular interaction via hydrogen bonding (Termonia et al., 1985). In *Bombyx*, the transcript size is 15 kb (Ohshima and Suzuki, 1977), which is approximately an order of magnitude larger than the *Antipaluria* fibroin transcript. This suggests that the much smaller protein size of the *Antipaluria* fibroin may explain the lower tensile strength of *Antipaluria* silk compared to *Bombyx* silk.

In summary, we characterized the molecular and mechanical properties of *Antipaluria urichi* silk. This silk has remarkably convergent similarities and surprising differences in comparison to other arthropod silks. Like many silks (e.g., Chang et al., 2005; Ayoub et al., 2007), embiid silk is dominated by glycine, alanine, and serine (Fig. 5) and is encoded by a transcript with a highly skewed codon usage (Table 2). We suggest that this codon usage bias in fibroin genes is important for minimizing the possibility of frame shift mutations within these highly repetitive sequences. Also, the *Antipaluria* carboxyl-terminal region has paired cysteine residues that have analogs, which are necessary for fiber formation, in the *Bombyx mori* HC fibroin (Fig. 4C; Inoue et al., 2000). Despite these similarities, *Antipaluria* silk has lower tensile strength and toughness compared to convergently evolved silks (Gosline et al., 2002; Chang et al., 2005; Swanson et al., 2006). These differences in tensile properties may be largely explained by the effects of molecular weight on tensile strength. By investigating both the tensile properties, encoding transcript and transcript size of *Antipaluria* silk, we gain insight into the functional significance of the embiid fibroin sequence elements. Webspinners are vitally dependent on their silk and they possess a radically different spinning system from the more frequently studied moths and spiders. Examining convergently evolved silks highlights recurring themes in the evolution of these adaptive molecules.

## Acknowledgements

We thank Edina Camama, Shou-Wei Ding, and Samer Elkashef for laboratory assistance. Nadia Ayoub, Merri Lynn Casem, John Gatesy, Michael McGowen, Morris Maduro, and Brook Swanson provided helpful comments. This research was supported by NSF awards DEB-0515868 to CYH and DEB-0515865 to JSE.

## References

Abramoff, M.D., Magelhaes, P.J., Ram, S.J., 2004. Image processing with Image J. Biophotonics Int. 11, 36–42.
Alberti, G., Storch, V., 1976. Ultrastructural investigations on silk glands of Embioptera. Zool. Anz. 197, 179–186.
Ayoub, N.A., Garb, J.E., Tinghitella, R.M., Collin, M.A., Hayashi, C.Y., 2007. Blueprint for a high-performance biomaterial: full-length spider dragline silk genes. PLoS ONE 2, e514.
Beuken, E., Vink, C., Bruggeman, C.A., 1998. One-step procedure for screening recombinant plasmids by size. Biotechniques 24, 748–750.
Beutel, R.G., Gorb, S.N., 2001. Ultrastructure and attachment specializations of hexapods (Arthopoda): evolutionary patterns inferred from a revised ordinal phylogeny. J. Zool. Syst. Evol. Res. 39, 177–207.
Blackledge, T.A., Cardullo, R.A., Hayashi, C.Y., 2005. Polarized light microscopy, variability in spider silk diameters, and the mechanical characterization of spider silk. Invertebr. Biol. 124, 165–173.
Blackledge, T.A., Hayashi, C.Y., 2006a. Silken toolkits: biomechanics of silk fibers spun by the orb web spider *Argiope argentata* (Fabricius 1775). J. Exp. Biol. 209, 2452–2461.
Blackledge, T.A., Hayashi, C.Y., 2006b. Unraveling the mechanical properties of composite silk threads spun by cribellate orb-weaving spiders. J. Exp. Biol. 209, 3131–3140.
Brown, S.A., Ruxton, G.D., 2004. Physical properties of *Hydropsyche siltalai* (Trichoptera) net silk. J. North Am. Benthol. Soc. 23, 771–779.
Chang, J.C., Fletcher, M.J., Gurr, G.M., Kent, D.S., Gilbert, R.G., 2005. A new silk: mechanical, compositional, and morphological characterization of leafhopper (*Kahaono montana*) silk. Polymer 46, 7909–7917.
Craig, C.L., 1997. Evolution of arthropod silks. Annu. Rev. Entomol. 42, 231–267.
Ding, S.-W., Li, W.-X., Symons, R.H., 1995. A novel naturally occurring hybrid gene encoded by a plant RNA virus facilitates long distance virus movement. EMBO J. 14, 5762–5772.
Edgerly, J.S., 1987a. Colony composition and some costs and benefits of facultatively communal behavior in a Trinidadian webspinner, *Clothoda urichi* (Embiidina: Clothodidae). Ann. Entomol. Soc. Am. 80, 29–34.
Edgerly, J.S., 1987b. Maternal behavior of a webspinner (Order Embiidina). Ecol. Entomol. 12, 1–11.
Edgerly, J.S., Davilla, J.A., Schoenfeld, N., 2002. Silk spinning behavior and domicile construction in webspinners. J. Insect Behav. 15, 219–242.
Engel, M.S., Grimaldi, D.A., 2006. The earliest webspinners (Insecta: Embiodea). Am. Mus. Novit. 3514, 1–15.
Fedič, R., Žurovec, M., Sehnal, F., 2003. Correlation between fibroin amino acid sequence and physical silk properties. J. Biol. Chem. 278, 35255–35264.
Garb, J.E., Hayashi, C.Y., 2005. Modular evolution of egg case silk genes across orb-weaving spider superfamilies. Proc. Natl. Acad. Sci. USA 102, 11379–11384.
Garb, J.E., DiMauro, T., Vo, V., Hayashi, C.Y., 2006. Silk genes support the single origin of orb webs. Science 312, 1762. 1762.
Gatesy, J., Hayashi, C., Motriuk, D., Woods, J., Lewis, R., 2001. Extreme diversity, conservation, and convergence of spider silk fibroin sequences. Science 291, 2603–2605.
Gorb, S.N., Niederegger, S., Hayashi, C.Y., Summers, A.P., Vöetsch, W., Walther, P., 2006. Silk-like secretion from tarantula feet. Nature 443, 407. 407.
Gosline, J., Guerettte, P.A., Ortlepp, C.S., Savage, K.N., 1999. The mechanical design of spider silks: from fibroin sequence to mechanical function. J. Exp. Biol. 202, 3295–3303.
Gosline, J., Lillie, M., Carrington, E., Guerette, P., Ortlepp, C., Savage, K., 2002. Elastic proteins: biological roles and mechanical properties. Philos. Trans. R. Soc. Lond. B Biol. Sci. 357, 121–132.
Hallam, M.A., Cansfield, D.L.M., Ward, I.M., Pollard, G., 1986. A study of the effect of molecular weight on the tensile strength of ultra-high modulus polyethylenes. J. Mater. Sci. 21, 54199–54205.
Hayashi, C.Y., Shipley, N.H., Lewis, R.V., 1999. Hypotheses that correlate the sequence, structure, and mechanical properties of spider silk proteins. Int. J. Biol. Macromol. 24, 271–275.
Higgins, L.E., White, S., Nuñez-Farfán, J., Vargas, J., 2007. Patterns of variation among distinct alleles of the *Flag* silk gene from *Nephila clavipes*. Int. J. Biol. Macromol. 40, 201–216.
Inoue, S., Tanaka, K., Arisaka, F., Kimura, S., Ohtomo, K., Mizuno, S., 2000. Silk fibroin of *Bombyx mori* is secreted, assembling a high molecular mass elementary unit consisting of H-chain, L-chain, and P25, with a 6:6:1 molar ratio. J. Biol. Chem. 275, 40517–40528.
Ittah, S., Cohen, S., Garty, S., Cohn, D., Gat, U., 2006. An essential role for the C-terminal domain of a dragline spider silk protein in directing fiber formation. Biomacromolecules 7, 1790–1795.

Lawrence, B.A., Vierra, C.A., Moore, A.M.F., 2004. Molecular and mechanical properties of major ampullate silk of the black widow spider, *Latrodectus hesperus*. Biomacromolecules 5, 689–695.

Merritt, D.J., 2007. The organule concept of insect sense organs: sensory transduction and organule evolution. Adv. Insect Physiol. 33, 192–241.

Murray, E.E., Lotzer, J., Eberle, M., 1989. Codon usage in plant genes. Nucleic Acids Res. 17, 477–498.

Nagashima, T., Niwa, N., Okajima, S., Nonaka, T., 1991. Ultrastructure of silk gland of webspinners *Oligotoma japonica* (Insecta, Embioptera). Cytologia 56, 679–685.

Nirmala, X., Mita, K., Vanisree, V., Žurovec, M., Sehnal, F., 2001. Identification of four small molecular mass proteins in the silk of *Bombyx mori*. Insect Mol. Biol. 10, 437–445.

Ohshima, Y., Suzuki, Y., 1977. Cloning of the silk fibroin gene and its flanking sequences. Proc. Natl. Acad. Sci. USA 74, 5363–5367.

Pérez -Rigueiro, J., Viney, C., Llorca, J., Elices, M., 1998. Silkworm silk as an engineering material. J. Appl. Polym. Sci. 70, 2439–2447.

Rocha, E.P.C., 2004. Codon usage bias from tRNA's point of view: redundancy, specialization, and efficient decoding for translation optimization. Genome Res. 14, 2510. 2510.

Ross, E.S., 1957. The Embioptera of California. Bull. Calif. Insect Survey 6, 51–57.

Ross, E.S., 2000. Contributions to the biosystematics of the insect order Embiidina. Part 1. Origin, relationships and integumental anatomy of the insect order Embiidina. Occas. Pap. Calif. Acad. Sci. 149, 1–53.

Sehnal, F., Žurovec, M., 2004. Construction of silk fiber core in Lepidoptera. Biomacromolecules 5, 666–674.

Sponner, A., Vater, W., Rommerskirch, W., Vollrath, F., Unger, E., Grosse, F., Wiesshart, K., 2005. The conserved C-termini contribute to the properties of spider silk fibroins. Biochem. Biophys. Res. Commun. 338, 897–902.

Sugiura, S., Yamazaki, K., 2006. The role of silk threads as lifelines for caterpillars: pattern and significance of lifeline-climbing behaviour. Ecol. Entomol. 31, 52–57.

Sutherland, T.D., Young, J.H., Sriskantha, A., Weisman, S., Okada, S., Haritos, V.S., 2007. An independently evolved dipteran silk with features common to lepidopteran silks. Insect Biochem. Mol. Biol. 37, 1036–1043.

Swanson, B.O., Blackledge, T.A., Beltran, J., Hayashi, C.Y., 2006. Variation in the material properties of spider dragline silk across species. Appl. Phys. Mater. Sci. Process 82, 213–218.

Taylor, J.S., Breden, F., 2000. Slipped-strand mispairing at noncontiguous repeats in *Poecilia reticulata*: a model for minisatellite birth. Genetics 155, 1313–1320.

Termonia, Y., 1994. Molecular modeling of spider silk elasticity. Macromolecules 27, 7378–7381.

Termonia, Y., 2006. Puncture resistance of fibrous structures. Int. J. Impact Eng. 32, 1512–1520.

Termonia, Y., Meakin, P., Smith, P., 1985. Theoretical study of the influence of molecular weight on the maximum tensile strength of polymer fibers. Macromolecules 18, 2246–2252.

Terry, M.D., Whiting, M.F., 2005. Mantophasmatodea and phylogeny of the lower neopterous insects. Cladistics 21, 240–257.

Trancik, J.E., Czernuszka, J.T., Bell, F.I., Viney, C., 2006. Nanostructural features of a spider dragline silk as revealed by electron and X-ray diffraction studies. Polymer 47, 5633–5642.

Ueda, H., Mizuno, S., Shimura, K., 1985. Sequence polymorphisms around the 5′-end of the silkworm fibroin H-chain gene suggesting the occurrence of crossing-over between heteromorphic alleles. Gene 34, 351–355.

Warwicker, J.O., 1960. Comparative studies of fibroins 2. Crystal structures of various fibroins. J. Mol. Biol. 2, 350–362.

Yonemura, N., Sehnal, F., 2006. The design of silk fiber composition in moths has been conserved for more than 150 million years. J. Mol. Evol. 63, 42–53.

Young, J.H., Merritt, D.J., 2003. The ultrastructure and function of the silk-producing basitarsus in the Hilarini (Diptera: Empididae). Arthropod Struct. Dev. 32, 157–165.

Žurovec, M., Kodrik, D., Yang, C., Sehnal, F., Scheller, K., 1998. The P25 component of *Galleria* silk. Mol. Gen. Genet. 257, 264–270.